Uniform Flux Heat Transfer to a Gas in Laminar Forced Convection in a Circular Tube

PERRY D. BERGMAN and LOWELL B. KOPPEL

Purdue University, Lafayette, Indiana

Heat transfer from a circular tube to a contained gas in laminar forced convection was studied dimensionally and experimentally. The boundary condition of uniform heat flux was physically achieved, and the experiments were conducted in a statistically designed pattern. The dimensional analysis, based upon the principle of corresponding states, and more general than any hitherto proposed, indicated four independent variables in this experiment. Of these, only bulk velocity showed a statistically significant effect in the region studied: a reduction in heat transfer coefficient with decreasing bulk velocity. No existing theories could explain this effect.

LITERATURE SURVEY

The problem of laminar flow heat transfer to a gas in a circular tube with a prescribed wall heat flux has been a subject of recent theoretical and experimental inquiry. Much of the discrepancy between theory and measurements in these studies arises from the inability to assess properly the role of variable physical properties in heat transfer. For the idealized case of constant fluid properties, the problem has been solved by Sellars et al. (*18*) and Siegel et al. (*19*). For a gas with variable physical properties, several theoretical solutions have been promulgated. Deissler (*3*) examined the problem of fully developed laminar flow of a gas with uniform wall heat flux (UHF). Viscosity and thermal conductivity were taken as being proportional to a power of temperature, while density was assumed to vary inversely with temperature. The two major assumptions made by Deissler were: the velocity at any radial distance does not depend on axial distance along the tube, and the radial equation of motion can be ignored and the radial velocity component is zero. The first assumption is correct only for no density change in the axial direction, and so is valid only for extremely low rates of heating. Koppel and Smith (*14*) have shown the fallacy of the second assumption by proving that it leads to the conclusion that velocity profiles can be calculated without recourse to the momentum equation, and the calculated profiles are independent of the gravity field. This assertion conflicts with the experimental results of Hanratty, Rosen, and Kabel (*4*), and Scheele and Hanratty (*17*). Thus, a radial velocity component must exist. Koppel and Smith (*14*) considered the laminar flow UHF problem for the entire thermal regime and solved the continuity equation and energy equation for variable specific heat and thermal conductivity, assuming a zero radial velocity. Their numerical results were for supercritical carbon dioxide.

Davenport and Leppert (*2*) considered the effect of a radial velocity component on heat transfer and fluid flow by postulating that the radial convective heat flux was equal to the negative product of the radial conductive heat flux, and a function of radial distance. Expressed mathematically, this means that

$$\rho v C_p T = R(r) k \frac{\partial T}{\partial r} \tag{1}$$

The function $R(r)$ must lie between zero and one. If $R(r)$ were unity, this would imply that no energy was being transmitted to the fluid by axial bulk convection, which would be an absurdity. In addition, v must vanish at the wall, and at the centerline must satisfy $\partial v/\partial r = 0$. Davenport and Leppert then included the temperature dependencies of k, μ, and ρ for nitrogen and helium, and solved the equations of change numerically for various forms of $R(r)$. Rigorously speaking, this approach is incorrect. Equation (1) is actually a simplified version of the energy equation,

$$\frac{1}{r}\frac{\partial}{\partial r}\left(kr\frac{\partial T}{\partial r} + \rho C_p v T r \right) = \rho u C_p \frac{\partial T}{\partial x} \tag{2}$$

A true solution to the problem would involve a simultaneous solution of the continuity equation, the radial and axial momentum equations, and the energy equation, with suitable assumptions.

Worsøe-Schmidt and Leppert (*21*) have recently undertaken such a solution. They utilize the simpler boundary-layer equations rather than the complete equations for tubular flow, but do include radial and axial velocities and variation of physical properties. The continuity, momentum, and energy equations were solved by finite-difference methods for a variety of boundary conditions and operating conditions, including the UHF condition studied in the present work. When Nusselt numbers were based on thermal conductivity evaluated at the local mixed mean temperature, they report "surprisingly small deviations from the solution for constant physical properties."

Experimental data on this problem are sparse; liquid UHF observations have been more plentiful than gas observations (*4* to *6*, *11*, *17*). This is because gases are extremely poor heat transfer media. They have low thermal conductivities and densities and slow gas mass flow rates are needed to remain within the laminar region. Thus, the heat transfer capacities of gases in laminar flow are quite low and transfers of heat to the gas are of the same order of magnitude as transfers to the insulation surrounding the test section. Another problem in gas flow is the difficulty of measuring accurately the temperature of a low-

Perry D. Bergman is with the U. S. Army Biological Laboratory, Frederick, Maryland.

velocity gas. However, the effect of variable properties is most significant for gases; hence the desire to conduct experiments on gases.

Kays and Nicoll (*10*) and Davenport and Leppert (*2*) attempted to mitigate the insulation heat leak problem by making accurate estimates of heat losses. To accomplish this, Kays and Nicoll performed a series of empty section tests, which permitted the construction of a plot of local heat loss as a function of local wall-to-surroundings temperature difference. Davenport and Leppert do not state how they correct for heat losses, but their method may be assumed similar to that of Kays and Nicoll. Local heat input during heat transfer tests is determined by subtracting the local heat leak thus measured from the total electrical heat input. In view of the two- and possibly three-dimensional nature of the heat leak problem, it is difficult to justify the use of measurements such as empty section tests and insulation temperatures as primary sources of experimental information, particularly since the indicated corrections are of the same order of magnitude as the heat fluxes. With this technique, it is impossible to obtain the UHF boundary condition. The closest analytical approximation to the heat flux distribution actually obtained is an initial step increase in heat flux at the test section entrance, followed by a negative ramp over the rest of the tube. This change in boundary condition may be presumed to affect the measured heat transfer coefficient.

Superficially, at least, it appears that by working with small-diameter tubes, natural convection effects may be eliminated. According to Scheele and Hanratty (*17*), a velocity profile in upflow heating develops an inflection point at a N_{Gr}/N_{Re} value greater than 32.94. With this criterion, no free convection effects should appear in the experiments of Kays and Nicoll, Davenport and Leppert, or in the present experiments. In fact, for nitrogen at flow rates and physical conditions typical of those used in all experiments, it is necessary to have a wall flux of 1,000 B.t.u./(hr.)(sq. ft.) in a tube with 0.7-in. I.D. to achieve N_{Gr}/N_{Re} values in excess of the critical value (*1*). These conditions were not approached in any reported experiments.

DIMENSIONAL ANALYSIS

One of the primary difficulties surrounding variable physical properties problems is the lack of any universal dimensional analysis which is valid for all fluids. The standard heat transfer correlations for heating or cooling of fluids in tubes typically employ the following dimensionless groups: Nusselt number, Prandtl number, and Reynolds number. Other groups, such as the Grashof number and the viscosity ratio (μ_b/μ_w), arise from considering linear departures from constant property behavior (*1*).

The inadequacy of existing methods of heat transfer correlation is revealed by a cursory survey of the recent literature. For example, the data of Koppel and Smith (*12, 13*) and of Wood and Smith (*20*) reveal anomalous heat transfer behavior in the neighborhood of the critical point, because of the rapid change taking place in transport properties. These data cannot be correlated by any of the standard heat transfer groups. There has also been considerable dispute over studies of forced convection heat transfer to hydrogen in the supercritical region (*8, 9*) as to what constitutes a satisfactory method of correlating data. Even for the well-investigated variable-properties experiment on turbulent flow of gases in tubes, a question exists as to whether a temperature-dependent Nusselt type of correlation actually describes the effect of thermal and transport property variations on the heat transfer process (*15*).

The principle of corresponding states has long been used to predict the transport and equilibrium properties of pure substances. The principle, in its most general form, asserts that if two different substances have identical values for two reduced variables, they have approximately identical values for a third. Pitzer (*7*) and Helfand and Rice (*16*) have furnished a statistical mechanical proof of the corresponding states principle. These proofs are predicated on the assumption that the intermolecular potential is of the form

$$\phi = \epsilon\,\phi'\,(r'/\sigma) \qquad (3)$$

For substances to obey closely the corresponding states hypothesis, they should have molecules with similar intermolecular force potential and thus be members of the same chemical family.

When using the corresponding states hypothesis, a more general dimensional analysis than hitherto achieved is possible. This analysis is presented in reference *1*, and involves the use of the critical constants T_c, P_c, ρ_c, V_c, μ_c and k_c to nondimensionalize T, P, ρ, V, μ, and k; the specific heat evaluated at zero pressure and the critical temperature $C^\circ{}_{p_c}$ to nondimensionalize C_p; u_{b_o} to nondimensionalize velocities and time; and D to nondimensionalize distances. The advantage of this approach is that the variable physical properties appear as reduced quantities and should be the same functions of the reduced temperature and pressure for all substances obeying the corresponding states principle.

The results of the dimensional analysis indicate that the critical Nusselt number hD/k_c is a function of nine independent dimensionless groups:

$$\frac{hD}{k_c} = g\left(x^*, \frac{P_c}{\rho_c u_{bo}{}^2}, \frac{Du_{bo}\rho_c}{\mu_c}, \frac{gD}{u_{bo}{}^2}, \frac{z_cR}{C^\circ{}_{p_c}M}, \frac{C^\circ{}_{p_c}\mu_c}{k_c}, T_o^*, P_o^*, \frac{q_wD}{k_cT_c}\right) \qquad (4)$$

Admittedly, the analysis is limited by the validity of the corresponding states principle, the fact that the fluids involved must have identical zero pressure C_p-T relationships, and the lack of information about physical properties. However, the previous methods of correlation cannot cope with large physical property variations (except in highly specific terms), necessitate the evaluation of physical properties at some predetermined reference temperature to create agreement with constant property theory, and have no theoretical justification.

INSULATION THEORY

A major purpose of this research was to construct a system in which the analytical boundary condition of constant wall heat flux could be realized. To achieve this objective, test section heat losses must be minimized. The data of previous investigations indicate the inadequacy of insulating the test section with commercially available materials.

A possible solution is to use some form of insulation superior to Fiberglas or glass wool, such as a vacuum bottle or a powdered insulation under vacuum. Hallman (*5, 6*) used a vacuum bottle for his investigation of laminar flow heat transfer to water in a vertical circular tube. He found the effective k of his system to be about 0.0046 B.t.u./(hr.)(ft.)(°F.), compared with a value of 0.023 B.t.u./(hr.)(ft.)(°F.) for glass wool. For laminar flow of a gas, even this high degree of insulation leads to prohibitively large heat losses at the high temperature end of the tube. Another drawback of this method is the difficulty of bringing thermocouple wires and power leads through vacuum tight seals.

A second approach, and that adopted here, is suggested by the fact that the heat loss to the surroundings is directly proportional to $(T_w - T_s)$, and hence a near adiabatic condition for the system can be closely approximated by diminishing $(T_w - T_s)$ along the test section. This can be accomplished by reproducing as closely as possible the test section wall temperature profile on a surrounding concentric tube. The annulus between the two tubes was filled with vermiculite insulation to reduce the heat loss penalty for any temperature differences between corresponding insulation thermocouples and test section wall thermocouples. This method was found to yield close approximation to the UHF condition.

DESIGN OF EXPERIMENTS

From the dimensional analysis, hD/k_c is, in general, a function of nine dimensionless groups. To form a general correlation, an extensive experimental program covering many different gases, tube diameters, velocities, heat fluxes, and entrance conditions would be necessary.

Because of the difficulty of construction of the equipment, only one test section diameter was employed. It was also decided to conduct this study with a single gas, nitrogen. If two different gases are employed in a single tube, it becomes impossible to formulate situations in which a significant number of dimensionless groups can be held constant while those of interest are varied.

From Equation (4) it can be seen that, for a single gas flowing through a test section of known diameter, there are only four variables which can affect hD/k_c at a given location. These are T_o^*, P_o^*, $q_wD/(k_cT_c)$, which appear as groups; and u_{bo}, which appears in three of the dimensionless groups. T_c, P_c, and k_c are constants for a given gas, so that T_o^*, P_o^*, and $q_wD/(k_cT_c)$ are referred to as T_o, P_o, and q_w throughout the remainder of this paper. Therefore, a set of experiments was planned to study the effects of these four variables on the heat transfer coefficient. A systematic and economical way to accomplish this is to study each one of the four factors at two different levels, that is, to conduct sixteen factorial experiments and to apply statistical principles to analyze the results.

SCOPE OF EXPERIMENTS

A number of conflicting factors must be balanced to arrive at a feasible experimental design: the possibility of transition to turbulent flow, too low wall-to-bulk temperature differences, a maximum operating temperature of 600° to 700°F. for copper-constantan thermocouples, the fact that the limits on P_o and T_o indirectly determine the limits on u_{bo}, and safety considerations. Therefore, the variables in the experimental design were investigated in a two-level factorial experiment at the following levels: T_o : 530° and 580°R. (spread of 10%). q_w : 80 and 105 B.t.u./(hr.)(sq.ft.) (spread of 30%). P_o : 85 and 105 lb./sq.in.abs. (spread of 25%). u_{bo} : 2.0 and 2.5 ft./sec. (spread of 20%).

It will be noted that the ranges of variation of these variables, in terms of percentage change, are small. Therefore, if it is found from statistical analysis of the results that a particular variable has no effect on the heat transfer coefficient, this statement can only apply to the small region studied. Such a statement may or may not be of interest. However, if a particular variable is statistically demonstrated to have an effect, then the size of the region studied is unimportant, except for estimation of the quantitative magnitude of the effect.

EQUIPMENT AND PROCEDURE

An overall flow diagram, an overall electrical diagram, and mixing chamber details are shown in Figures 1, 2, and 3. Pressurized gas flowed from a cylinder to a 30-ft. length of ¼-in. O.D. stainless steel coil immersed in a well-stirred, constant-temperature bath. After leaving the coil, the gas flowed vertically upward through a 10-ft.-long, 0.250-in. O.D. Inconel test section that had a wall thickness of 0.0255 in. Inconel was used because of its low thermal coefficient of electrical resistivity, thus insuring the UHF condition. The first 3 ft. of the test section were submerged in the bath and served as a velocity entrance section. The final 7 ft. acted as an electrical resistance heater, heating the gas by uniform dissipation of electrical energy supplied to the test section. The test section was isolated from the surroundings by means of two electrically insulating stainless steel flanges. Test section wall temperatures were measured by a series of spot-welded copper-constantan thermocouples at different axial locations. The voltage across the test section was measured with an a.c. voltmeter. Together with the known value of the test section resistance (determined with a Kelvin bridge), this enabled evaluation of the power input to the test section. Temperatures were observed on a Rubicon Portable Precision Potentiometer, accurate to ± 0.005 mv. The entrance pressure of the gas was observed on a calibrated Ashcroft Bourdon tube gauge.

On leaving the test section, the gas passed through a mixing chamber where its bulk temperature was measured with a bare, 30-gauge, copper-constantan thermocouple suspended in the mixing chamber. This mixing chamber consisted of a porous, sintered stainless steel disk and a bed of alumina

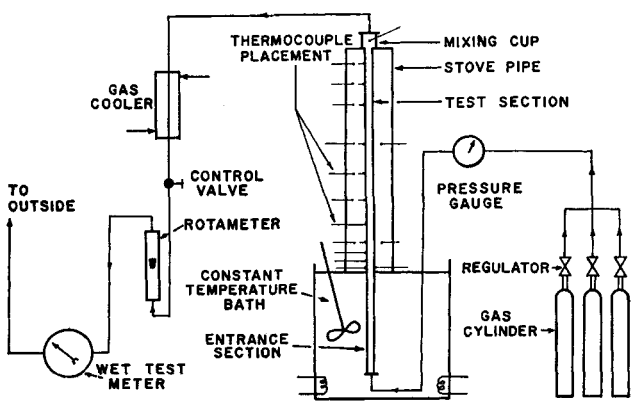

Fig. 1. Flow diagram of equipment.

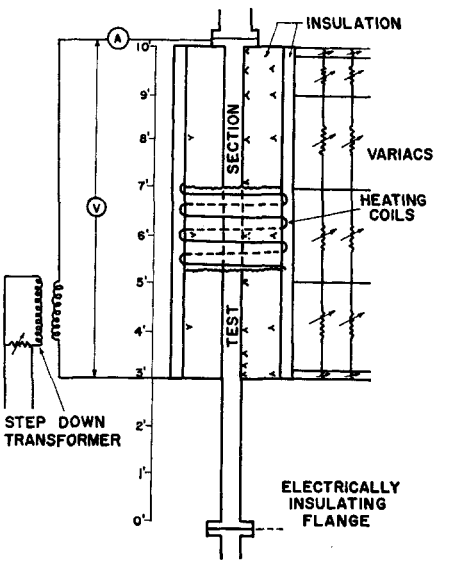

Fig. 2. Electrical diagram of heat transfer system.

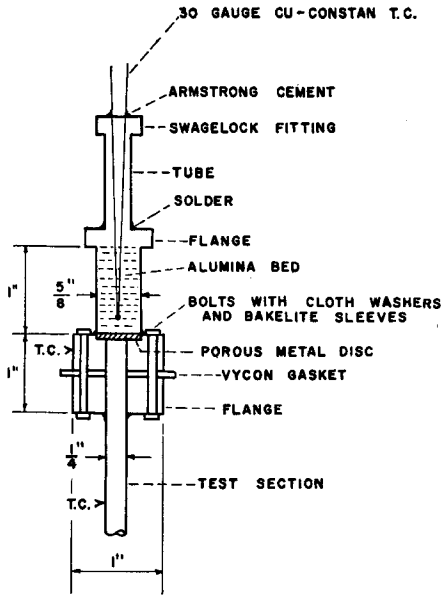

Fig. 3. Mixing chamber.

beads, as shown in Figure 3. The exit gas was then cooled in a countercurrent heat exchanger, and throttled by a high-pressure valve. It went through a rotameter and a wet test meter, where the volume of gas flowing through the meter in a given time interval was measured to give the reported flow rate. The rotameter was used only for manual flow rate control. The gas was then vented to the atmosphere.

The test section was surrounded by a 4-in. O.D. stove pipe filled with vermiculite insulation. The stove pipe was covered with aluminum foil to improve the thermal conductivity of the surface, then Chromolox Thermowire was uniformly wrapped around the stove pipe in six sections. These six auxiliary heaters were covered with Fiberglas insulation. Thermocouples were inserted ¼ in. into the vermiculite bed at the midpoint of each heating section. At this point, it was thought that the temperatures measured would be most characteristic of the particular heating section. The power input to each heater was regulated by two 7.5 amp. power-stats connected in series.

Five auxiliary heaters were adjusted to reduce radial heat losses by duplicating as closely as possible the test section temperature profile along the stove pipe. One auxiliary heater was adjusted to reduce axial heat losses at the test section exit.

A typical experimental run was conducted in the following fashion: First, a rough estimate of test section wall temperatures was made from the constant properties analytical solution. The auxiliary heaters were adjusted to these calculated values. Bath temperature, entrance pressure, gas flow rate, and wall heat flux were adjusted to the predetermined values. As steady state was approached (4 to 7 hr.) the power inputs to the auxiliary heaters were continually adjusted to bring the two sets of measured temperatures as close together as possible, less than 2°F. in all cases. A Honeywell Brown Electronik eight-point recorder was used to determine when the thermal system had reached steady state. Finally, readings were taken of all experimental quantities.

EXPERIMENTAL RESULTS

Sixteen factorially designed experiments, together with four duplications, were performed. A typical run is plotted in Figure 4. Wall temperatures were measured directly and bulk temperatures were determined by the following heat balance:

$$(H_b - H_{bo}) = (H_{bf} - H_{bo})\frac{x}{L} \qquad (5)$$

Local heat transfer coefficients were determined from the definition

$$h = \frac{q_w}{(T_w - T_b)} \qquad (6)$$

where

$$q_w = \frac{wc_p(T_{bf} - T_{bo})}{\pi DL} \qquad (7)$$

The graph exhibits two important qualitative trends. First, a thermal entrance region approximately 6 in. to 1 ft. in extent is indicated, followed by a region of approximately linear wall temperatures. Second, the bulk temperature profiles are approximately parallel to the wall temperature profiles, except over the thermal entrance region and the last 6 in. of the tube, where end effects occur. Thus, there is a locally fully developed thermal region between the entrance and end regions, in which h changes gradually with length, the change being inversely proportional to the change in the distance between the wall and bulk temperature profiles.

The experimental results were examined by several analyses of variance tests (ANOVA) to determine which of the independent variables (T_o, P_o, q_w, and u_{bo}) were statistically important. The selection of a dependent variable was not as clear-cut. h, in the locally fully developed region, stays between 3 to 5 B.t.u./(hr.)(sq.ft.)(°F.) and thus is not very sensitive to changes in experimental parameters. It was believed that $\Delta h = h - h_{cp}$ would provide a better measure of the influence of the experimental variables. The quantity h_{cp} is evaluated from the theoretical solution to the UHF problem with constant physical properties. Thus, both h and Δh were considered as dependent variables. To reduce the effect of thermocouple calibration errors, h used for the ANOVA tests was evaluated by averaging the values of h measured at

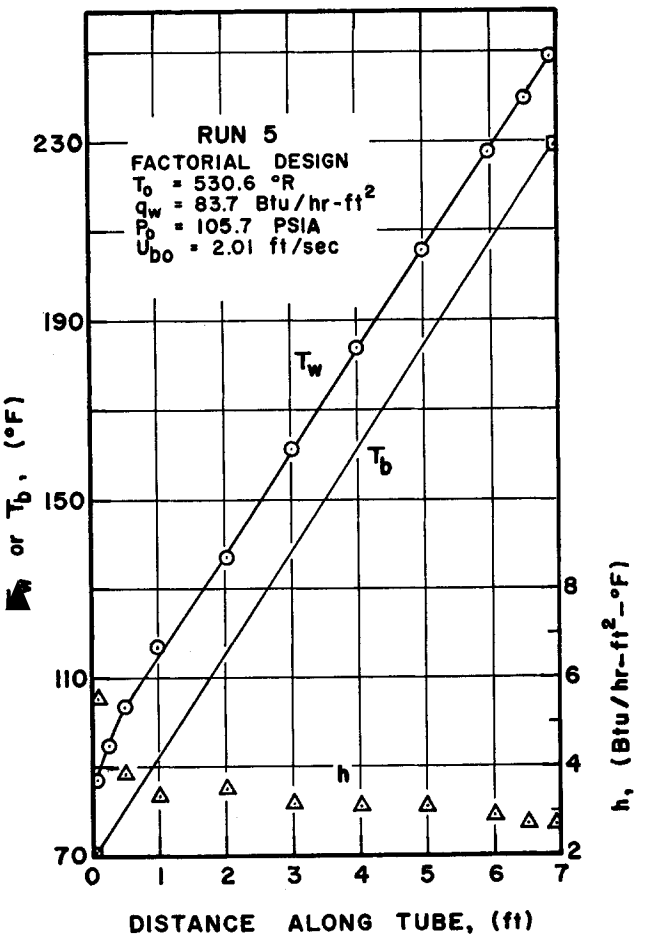

Fig. 4. Typical experimental results.

Table 1. ANOVA Results with Δh as Dependent Variable and Four Replicates

Source	Degrees of freedom	Sum of squares, [B.t.u./(hr.) (sq. ft.)(°F.)]^2	Mean square, [B.t.u./(hr.) (sq. ft.)(°F)]^2	F ratio
Pressure	1	0.342	0.342	3.93
Heat flux	1	0.005	0.005	0.057
Temperature	1	0.095	0.095	1.09
Velocity	1	1.202	1.202	13.8
Error	15	1.314	0.0874	
Total	19	2.958	1.7314	

$F_{0.75}(1,15) = 1.43$ $F_{0.90}(1,15) = 3.07$ $F_{0.99}(1,15) = 8.68$

1, 2, and 3 ft. downstream of the tube entrance (thermocouples with least experimental uncertainty).

ANOVA tests were performed for four cases: case A-16 runs, h dependent variable; case B-20 runs, h dependent variable; case C-16 runs, Δh dependent variable; case D-20 runs, Δh dependent variable. Cases with twenty runs included four replicates. The results of case D are shown in Table 1. In all cases, u_{bo} was significant at a 5% level or lower. In case A, q_w was significant at a 25% level; in cases B and D, P_o was significant at 10 and 25% levels. Therefore, u_{bo} exerts a definite influence on h. No concrete conclusions can be made concerning the significance of the other three variables. They are probably insignificant (*in the region studied*), because even if all four variables were insignificant and the sum of squares consisted entirely of experimental error, then, probably one variable in four would appear significant at a 25% level. (This is from the definition of significance level: if there is no effect, there is a ¼ chance of being wrong and predicting an effect.)

For the four replications of the factorial design runs, it was found that the average experimental error (nonreproducibility in h) was ± 12%. The combining in Table 1 of the sums of squares due to pressure, heat flux, temperature, and error, and the computing of a mean square based on 18 deg. of freedom, yield a residual mean square of 0.097 not accounted for in the velocity effect and hence apparently caused by random errors. The standard error is the square root of this value, 0.31, and hence is 8% of the average heat transfer coefficient, 4.0 B.t.u./(sq.ft.)(hr.)(°F.), which compares with the 12% scatter in the replicated runs.

The importance of u_{bo} is further emphasized by employing the t distribution to make separate interval estimates of h for eight low-velocity runs and for eight high-velocity runs. The following results were obtained: for the low-velocity runs, the interval ($3.60 < h < 4.00$) contained the true average h with probability 95%, while for the high-velocity runs, this interval was ($4.13 < h < 4.58$). The interval estimates show the lack of overlap of the two sets of data. The magnitude of reduction in h is estimated at 13% for a 20% reduction in u_{bo}.

The velocity effect can be seen directly from the graph of h vs. x in Figure 5. In this figure, T_o, P_o, and q_w are constant, but u_{bo} is different for each set of points. Note that two of the runs shown here are outside the factorial design. It is evident that h decreases with lowered velocity. Over the entire range, the reduction in h is estimated at 40% for a 46% reduction in u_{bo}.

Figure 6 shows a plot of N_{Nu_o} vs. x_o^* wherein the factorial design points are compared with the theoretical solution for constant properties. Owing to the velocity effect, many of the factorial design points fall below the theoretical curve. The lowered values of N_{Nu_o} at the end of the tube are caused by end effects. Figure 7 shows the same results plotted as N_{Nu_b} vs. x_b^*. Note that Nusselt numbers measured at *all* wall thermocouples are included in Figures 6 and 7; this contrasts with the data used in ANOVA which included only the averages of measurements at 1, 2, and 3 ft. However, only data from runs in the factorial design and not data from the low-velocity runs and from the low heat flux runs to be discussed below are included in these graphs.

The possibility of verifying experimentally the analytical solutions for constant properties was examined. The difficulties in the precise measurement of h at low heat fluxes were enormous. As $T_w - T_b$ is of the order of 5° to 11°F., a degree or two change in this difference can produce sharp changes in the measured value of h. In

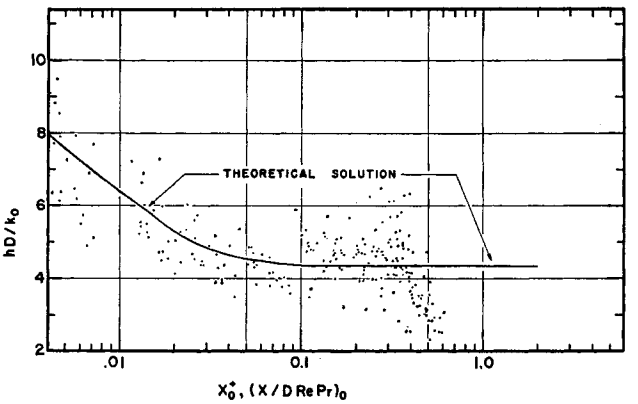

Fig. 6. N_{Nu_o} vs. x_o^* for factorial design.

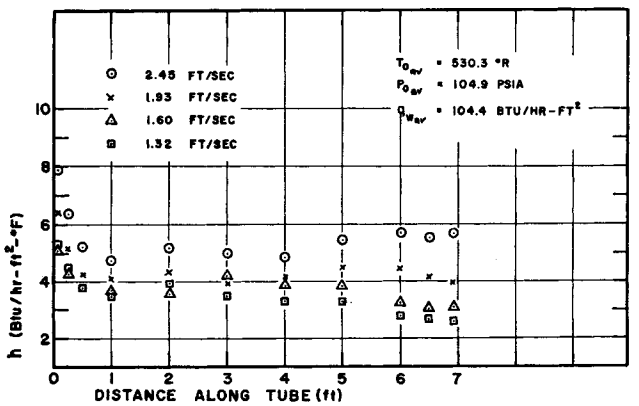

Fig. 5. Effect of velocity on heat transfer coefficient.

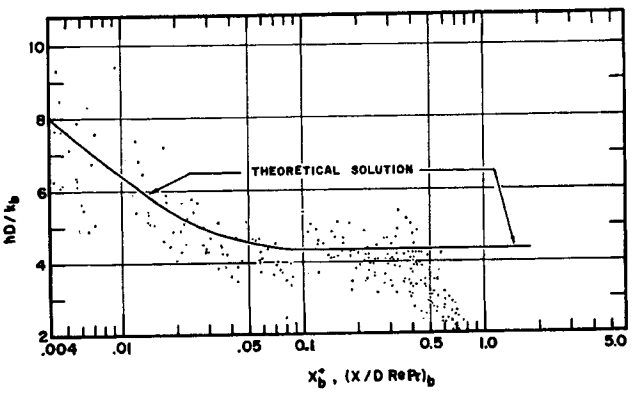

Fig. 7. N_{Nu_b} vs. x_b^* for factorial design.

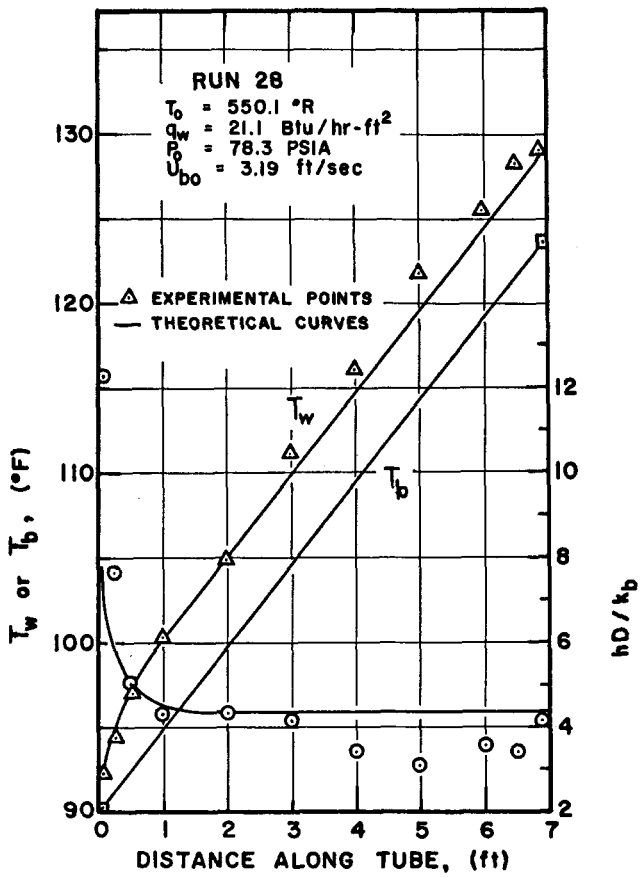

Fig. 8. Heat transfer results for low heat flux.

Figure 8 are plotted the results of one of two low heat flux runs taken. The results were encouraging in the sense that the theoretical assertions of the existence of two thermal regions and of the linearity of fully developed wall temperature profiles were definitely proved. The values of h do not allow firm quantitative conclusions; all that can be said in view of the large possible errors in h is that the data do not suggest any serious errors in the constant property solution.

EXPERIMENTAL ERRORS

The overall heat balance serves as a check on systematic errors by comparing the heat absorbed by the gas $wC_p\Delta T_b$ with the electrical heat input E^2/R_e. With the low heat fluxes realized experimentally, complete elimination of the discrepancy between the two heat estimates is impossible. In all the experiments reported here, the two heat estimates never differed by more than 15%; the average deviation was 8.4%. Kays and Nicol checked their results by a similar procedure. Davenport and Leppert did not measure the exit gas bulk temperature, so no heat balance check was possible. Axial conduction losses, a possible error in measuring the exit gas bulk temperature, errors in auxiliary heater adjustment, and the lack of perfect insulation all cause heat losses which can never be fully eliminated. For the present experiments, calculations placed an upper bound of 3% of the total heat input on the axial conduction losses.

COMPARISON WITH PREVIOUS EXPERIMENTAL WORK

Table 2 summarizes the experimental results of the three investigations reported in the literature. The bulk of the work of Kays and Nicoll and of Davenport and Leppert was conducted at high temperature ratios and high heat fluxes, because it was presumed that this was where the greatest departures from constant property theory would take place. The results reported in the present investigation were concentrated in a lower temperature ratio domain. Velocity effects were not detected in either of the previous investigations.

The present study had several advantages: (1) The UHF boundary condition was actually attained. (2) The design of the equipment made it possible to compare low heat flux data with the theoretical solution for constant properties. This is important because it served as a partial proof of equipment. (3) The factorial design permits more definitive conclusions to be reached. Thus, from Table 1 it may be stated that *there is less than one chance in one hundred that the observed effect of* u_{b_o} *is due to unfortunate random experimental errors.* (4) The more general dimensional analysis permitted elucidation of the relevant experimental variables.

Kays and Nicoll concluded from their results that, as the heat flux is raised, the Nusselt numbers more closely approach the theoretical solution for constant physical properties, an apparently anomalous result. However, no statistical tests were made to determine the confidence level of this conclusion. Owing to the scatter inherent in heat transfer measurements, statistical considerations are of prime importance. Furthermore, the Nusselt number compared was N_{Nu_b}, which includes the variation of k_b along the tube. The constant property solution uses a constant value of k, and a more rigorous comparison with this solution should use k_o in all Nusselt numbers, as is done in Figure 7. In addition, the previous investigations did not physically achieve the UHF condition; hence, their conclusion is not firmly based.

COMPARISON OF DATA WITH EXISTING THEORIES

Since a major result of the present investigation is the demonstration of the existence of a velocity effect, the

Table 2. Results of Investigations of Laminar Flow of Gas Heat Flux Problem

	Kays and Nicoll	Davenport and Leppert	Present research
Gas	Air	*a* Nitrogen *b* Helium	Nitrogen
No. of runs	6	8	24
T_w/T_b	1.01 to 1.87	*a* 1.0 to 2.2 *b* 1.0 to 1.8	1 to 1.13
w, lb./hr.	1.3	*a* 0.32 to 0.89 *b* 0.15 to 0.88	0.45 to 1.1
B.C.	Ramp heat flux	Ramp heat flux	UHF
Comments	N_{Nu_b} agrees with constant property solution	N_{Nu_b} agrees with constant property solution	N_{Nu_o} agrees with constant property solution at high velocities; disagrees at low velocities

theories of Deissler (3), Davenport and Leppert (2), and Koppel and Smith (14) were examined for prediction of this effect, without success (1). The first two theories showed effectively no change of N_{Nu} with u_{bo} for the conditions of the present experiment, while the last theory predicted a change in the incorrect direction. Worsøe-Schmidt and Leppert (21) did not investigate the specific effect of velocity on heat transfer coefficients. (In addition, their Nusselt numbers are based on the thermal conductivity evaluated at the local bulk temperature, as are the experimental values of Kays and Nicoll.) Thus, no satisfactory theoretical explanation has been found to explain quantitatively the observations.

Qualitatively, one can postulate that the reduction in heat transfer coefficient at low axial velocities is a result of the increasing importance of transverse radial convection, which Davenport and Leppert have suggested is pointed from the center of the tube to the wall. Worsøe-Schmidt and Leppert confirm this direction in the section of the tube beyond the thermal entrance length. However, the quantitative predictions of Davenport and Leppert have not been demonstrated to agree with the data, as discussed above.

Since the existence of a reduction in heat transfer coefficient with decreasing bulk velocity is indicated by the present experiments to exist beyond reasonable doubt, an adequate theoretical analysis will have to predict this effect.

ACKNOWLEDGMENT

The authors are grateful to the Procter and Gamble Company, Dow Chemical Company, and E. I. Du Pont de Nemours Company for their support of this work in the form of fellowships to P. D. Bergman.

NOTATION

C_p = specific heat at constant pressure, B.t.u./(lb.)(°F.)
C°_{pc} = zero pressure specific heat evaluated at critical temperature, B.t.u./(lb.)(°F.)
D = inside diameter of test section, ft.
E = voltage across test section, v.
F = test statistic with F distribution
g = gravitational acceleration, ft./sec.^{2}
H = enthalpy, B.t.u./lb.
H^o = enthalpy at zero pressure, B.t.u./lb.
H^* = reduced state enthalpy, $(H - H^\circ)_T/(RT_c)$, dimensionless
H_b = bulk enthalpy
H_{bf} = bulk enthalpy at test section exit
H_{bo} = bulk enthalpy at test section entrance
h = heat transfer coefficient, B.t.u./(hr.)(sq. ft.)(°F.)
h_{cp} = heat transfer coefficient given by analytical solution for constant physical properties
k = thermal conductivity, B.t.u./(hr.)(ft.)(°F.)
L = length of tube, ft.
M = molecular weight, lb./mole
N_{Gr} = Grashof number
N_{Nu_o} = Nusselt number with k evaluated at tube entrance
N_{Nu_b} = Nusselt number with k evaluated using local bulk temperature
N_{Pe} = Peclet number
N_{Pr} = Prandtl number
N_{Re} = Reynolds number
P = pressure, lb./sq. in. abs.
P^* = P/P_c
Pr = Prandtl number, dimensionless
q = total heat input, B.t.u./hr.
q_w = heat flux, B.t.u./(hr.)(ft.)
R = radius of test section, ft.
R = gas constant, (lb./sq. in. abs.)(cu. ft.)/(°R.)(lb.-mole)
$R(r)$ = function of radius, dimensionless
R_e = electrical resistance of test section, ohms
Re = Reynolds number, dimensionless
r = distance in radial direction, ft.
r' = distance between molecules, Å.
r^* = radial coordinate, r/D, dimensionless
T = temperature, °R.
T^* = T/T_c
t = time, sec.
t = test statistic with Student's distribution, dimensionless
t^* = time coordinate, tu_{bo}/D, dimensionless
$\mathbf{u}$ = velocity vector, ft./sec.
u_x = velocity in axial direction, ft./sec.
u_y = velocity in y direction, ft./sec.
u_z = velocity in z direction, ft./sec.
u_b = bulk velocity, ft./sec.
u_{bo} = bulk velocity evaluated at tube entrance, ft./sec.
v = radial velocity, ft./sec.
V = specific volume, cu. ft./lb.
w = mass flow rate, lb./hr.
x = distance along tube in axial direction, ft.
x^+ = distance parameter, $x/(DPe_b)$, dimensionless
x^* = x/D
y = rectangular coordinate, ft.
z = rectangular coordinate, ft.
z_c = critical compressibility factor, dimensionless

Greek Letters

ϵ = characteristic energy constant, ergs
μ = viscosity, lb./(ft.)(hr.)
ρ = density, lb./cu. ft.
σ = characteristic distance constant, Å.
ϕ = intermolecular potential, ergs
ϕ' = general function of r'/σ, dimensionless

Subscripts

b = quantity evaluated at the bulk condition
c = quantity evaluated at the critical point
cp = quantity evaluated by assuming constant properties
f = quantity evaluated at the tube exit
o = quantity evaluated at the tube entrance
T = quantity evaluated at constant temperature
w = quantity evaluated at inner wall of tube

Superscripts

$*$ = reduced quantity dimensionless
o = quantity at zero pressure

LITERATURE CITED

1. Bergman, P. D., Ph.D. thesis, Purdue Univ., Lafayette, Ind. (1965).
2. Davenport, M. E., and G. Leppert, *J. Heat Transfer*, **87C**, 191 (1965).
3. Deissler, R. G., *Natl. Advisory Comm. Aeronaut. Tech. Note 2410* (July, 1951).
4. Hanratty, T. J., E. M. Rosen, and R. L. Kabel, *Ind. Eng. Chem.*, **50**, 815 (1958).
5. Hallman, T. M., Ph.D. thesis, Purdue Univ., Lafayette, Ind. (1958).
6. ———, *Natl. Aeronaut. Space Admin. Tech. Note D-1104* (December, 1961).
7. Helfand E., and S. Rice, *J. Chem. Phys.*, **32**, 1642 (1960).
8. Hendricks, R. C., R. W. Graham, Y. Y. Hsu, and A. A. Mederios, *ARS J.*, **32**, 244 (1962).
9. Hess, M. L., and H. R. Kunz, *J. Heat Transfer*, **87C**, 41 (1963).
10. Kays, W. M., and W. B. Nicoll, *ibid.*, **85C**, 329.
11. Kemeny, G. A., and E. V. Somers, *ibid.*, **84C**, 339 (1962).

12. Koppel, L. B., Ph.D. thesis, Northwestern Univ., Evanston, Ill. (1960).
13. ———, and J. M. Smith, paper No. 69, 579, *Intern. Develop. Heat Transfer*, Am. Soc. Mech. Engrs. (1961).
14. ————, *J. Heat Transfer*, **84C**, 157 (1962).
15. McEligot, D. M., P. M. Magee, and G. Leppert, *ibid.*, **87C**, 67 (1965).
16. Pitzer, K. S., *J. Chem. Phys.*, **7**, 583 (1939).
17. Scheele, G. F., and T. J. Hanratty, *J. Fluid Mech.*, **14**, 244 (1962).
18. Sellars, J. R., M. Tribus, and J. S. Klein, *Trans. Am. Soc. Mech. Engrs.*, **78**, 441 (1956).
19. Siegel, R., E. M. Sparrow, and T. M. Hallman, *Appl. Sci. Res.*, **A7**, 386 (1958).
20. Wood, R. D., and J. M. Smith, *A.I.Ch.E. J.*, **10**, 180 (1964).
21. Worsøe-Schmidt, P. M., and G. Leppert, *Intern. J. Heat Mass Transfer*, **8**, 1281 (1965).

Paper received August 13, 1965; revision received January 19, 1966; paper accepted January 21, 1966.

The Surface Transport of Adsorbed Molecules

J. A. WEAVER and A. B. METZNER

University of Delaware, Newark, Delaware

A detailed mechanistic model is developed to describe the process by which adsorbed molecules migrate over the surface of an adsorbent. The migration is assumed to occur as a result of a random hopping of partially desorbed species; explicit expressions are derived for the hopping rate and the distance traversed in a single jump for the case of a gas adsorbed on a homogeneous surface. In the degree of detail developed herein experimental determinations are still required (to evaluate an otherwise unknown ratio of partition functions, and the activation free energy) but the pressure or surface concentration dependency of the transport rate is given explicity.

The predictions are tested by comparison with three sets of experimental data for hydrocarbons adsorbed on porous glass; these systems were chosen as they may be shown to meet the assumption of an adsorbate migrating over an energetically homogeneous surface under the conditions studied. Reasonable values are found for the parameters and excellent agreement between the observed and predicting trends with pressure is noted in all cases.

The transport of an adsorbate along a solid surface or through a porous solid is known to occur by several different mechanisms. In the case of a gas being transported through a porous solid, for example, the ratio of the mean free path in the gas phase to the width of the pores or cavities in the solid determines whether the gas phase transport corresponding to an imposed pressure gradient can be described by the Knudsen mechanism of free molecular flow, by the mechanism of viscous laminar flow, or by a combination of the two (*1, 5, 11, 15*). Furthermore, if the gas is adsorbed appreciably onto the solid, an additional transport due to the migration of the adsorbed gas on the inner surface of the porous solid must be considered (*4, 5*); it has been observed that for many systems the transport rate of the adsorbed phase is comparable to and sometimes greater than that of the gas phase (*1, 2, 7, 9, 16*). Therefore, an understanding of the transport characteristics of adsorptive solids (including porous adsorbents and catalysts, for example) requires consideration of surface transport mechanisms. Recent studies (*1* to *3, 9, 16*), while contributing to our knowledge of the subject, also reveal major limitations, especially in theoretical and predictive abilities. Thus, this work is directed toward an improved understanding of surface transport processes, primarily by means of a theoretical analysis. This analysis is evaluated by employing transport rate data for several adsorbing and nonadsorbing gases in a porous solid of known uniform structure.

J. A. Weaver is with Shell Development Company, Emeryville, California.

DERIVATION AND USE OF THE BASIC RATE EXPRESSION

The basic rate expression is expected to be applicable equally to porous adsorbents and to planar surfaces. Because the former may be of greater industrial interest they were chosen for use in the evaluation of the rate expressions and the details of the development herein will be directed accordingly.